α-Lipoic Acid Prevents Neointimal Hyperplasia Via Induction of p38 Mitogen-Activated Protein Kinase/Nur77-Mediated Apoptosis of Vascular Smooth Muscle Cells and Accelerates Postinjury Reendothelialization

Han-Jong Kim, Joon-Young Kim, Sun Joo Lee, Hye-Jin Kim, Chang Joo Oh, Young-Keun Choi, Hyo-Jeong Lee, Ji-Yeon Do, Sun-Yee Kim, Taeg-Kyu Kwon, Hueng-Sik Choi, Mi-Ock Lee, In-Sun Park, Keun-Gyu Park, Ki-Up Lee, In-Kyu Lee

Objective—To explore whether α-lipoic acid (ALA), a naturally occurring antioxidant, inhibits neointimal hyperplasia by inducing apoptosis of vascular smooth muscle cells and to examine its potential effects on reendothelialization and platelet aggregation.

Methods and Results—Restenosis and late stent thrombosis, caused by neointimal hyperplasia and delayed reendothelialization, are significant clinical problems of balloon angioplasty and drug-eluting stents. ALA treatment strongly induced apoptosis of vascular smooth muscle cells and enhanced the expression and cytoplasmic localization of Nur77, which triggers intrinsic apoptotic events. Small interfering RNA–mediated downregulation of Nur77 diminished this proapoptotic effect of ALA. Moreover, ALA increased p38 mitogen-activated protein kinase phosphorylation, and inhibition of p38 mitogen-activated protein kinase completely blocked ALA-induced vascular smooth muscle cell apoptosis and Nur77 induction and cytoplasmic localization. In balloon-injured rat carotid arteries, ALA enhanced Nur77 expression and increased TUNEL-positive apoptotic cells in the neointima, leading to inhibition of neointimal hyperplasia. This preventive effect of ALA was significantly reduced by infection of an adenovirus encoding Nur77 small hairpin (sh)RNA. Furthermore, ALA reduced basal apoptosis of human aortic endothelial cells and accelerated reendothelialization after balloon injury. ALA also suppressed arachidonic acid–induced platelet aggregation.

Conclusion—ALA could be a promising therapeutic agent to prevent restenosis and late stent thrombosis after angioplasty and drug-eluting stent implantation. **(*Arterioscler Thromb Vasc Biol*. 2010;30:2164-2172.)**

Key Words: apoptosis ■ α-lipoic acid ■ Nur77 ■ VSMC ■ neointimal hyperplasia

Restenosis caused by neointimal hyperplasia is a main obstacle in the long-term success of percutaneous coronary intervention, such as balloon angioplasty and stenting. Neointimal hyperplasia is characterized by diffuse intimal thickening, resulting from uncontrolled proliferation of vascular smooth muscle cells (VSMCs).[1–3] Along with excessive proliferation of VSMCs, decreased VSMC apoptosis also plays a crucial role in the development and progression of neointimal hyperplasia.[4–6] The intrinsic antiapoptotic phenotype, leading to diabetic vasculopathy, was observed in neointimal VSMCs isolated from patients with diabetes mellitus.[4] Inhibition of antiapoptotic B cell lymphoma-x (Bcl-x) expression induces VSMC apoptosis and reduces neointimal hyperplasia and intimal lesion formation.[5,6]

Drug-eluting stents (DESs), which locally release antiproliferative drugs, profoundly reduce the rate of in-stent restenosis.[3] However, late stent thrombosis (LST) associated with delayed reendothelialization remains a major problem, limiting the long-term efficacy and safety of DESs.[3,7] Delayed or incomplete reendothelialization contributes to neointimal hyperplasia, and accelerated reendothelialization inhibits restenosis and LST.[7–9] Therefore, pharmacological agents that inhibit proliferation and increase apoptosis in VSMCs while

Received on: January 21, 2010; final version accepted on: August 24, 2010.

From the Departments of Internal Medicine and Biochemistry and Cell Biology (H.-J.K., J.-Y.K., S.J.L., H.-J.K., C.J.O., H.-J.L., J.-Y.D., S.-Y.K., and I.-K.L.), Kyungpook National University School of Medicine, Daegu, Korea; the Department of Internal Medicine (Y.-K.C. and K.-G.P.), Keimyung University School of Medicine, Daegu, Korea; the Department of Immunology (T.-K.K.), Keimyung University School of Medicine, Daegu, Korea; the Hormone Research Center (H.-S.C.), School of Biological Sciences and Technology, Chonnam National University, Gwangju, Korea; the College of Pharmacy and Bio-MAX Institute (M.-O.L.), Seoul National University, Seoul, Korea; the Department of Anatomy and the Center for Advanced Medical Education by BK21 project (I.-S.P.), College of Medicine, Inha University, Incheon, Korea; and the Department of Internal Medicine (K.-U.L.), University of Ulsan College of Medicine, Seoul, Korea. Dr Hye-Jin Kim is now with the Metabolic Signal Research Center, Institute for Molecular and Cellular Regulation, Gunma University, Maebashi, Gunma, Japan.

Dr Han-Jong Kim, Dr Joon-Young Kim, and Sun Joo Lee contributed equally to this work.

Correspondence to In-Kyu Lee, MD, PhD, Department of Internal Medicine, Kyungpook National University School of Medicine, 50 Samduk-2Ga, Jung-Gu, Daegu 700-721, Korea. E-mail leei@knu.ac.kr

Arterioscler Thromb Vasc Biol **is available at http://atvb.ahajournals.org** **DOI: 10.1161/ATVBAHA.110.212308**

accelerating reendothelialization appear to be useful for the prevention of restenosis and LST after DES implantation.

Nur77, also known as nuclear receptor subfamily 4 group A member1 (NR4A1), nerve growth factor-induced clone B, and TR3, is a transcription factor that belongs to a nuclear hormone receptor superfamily.[10] Nur77 is implicated in both cell survival and apoptosis, depending on the cell types and agents used, although its precise physiological function is not yet fully understood. Nur77 is transiently induced by serum and growth factors and exerts mitogenic effects through its direct binding to a conserved DNA element and transactivation function in the nucleus.[11,12] It is also upregulated in response to diverse apoptotic stimuli and exhibits a proapoptotic action in T cells and cancer cell lines.[13–16] This proapoptotic feature of Nur77 is associated with its translocation from nucleus to mitochondria, where it interacts with Bcl-2.[17] This interaction, in turn, induces a conformational change in Bcl-2, leading to conversion of Bcl-2 from an antiapoptotic to a proapoptotic molecule to initiate apoptosis by triggering cytochrome C release from mitochondria. Overexpression or activation of Nur77 also protects against neointimal hyperplasia through inhibition of VSMC proliferation.[18,19] However, the physiological relevance of the proapoptotic role of Nur77 in neointimal hyperplasia has been poorly investigated.

α-Lipoic acid (1,2-dithiolane-3-pentanoic acid [ALA]), a naturally occurring powerful antioxidant, induces apoptosis of several tumor cell lines.[20–22] Several lines of evidence from clinical and experimental data also suggest that ALA could be used to prevent the development of atherosclerosis.[21,23] It was previously reported that ALA improves vascular dysfunction and prevents free fatty acid–induced apoptosis of vascular endothelial cells by activating AMP-activated protein kinase.[24] It was also demonstrated that ALA prevents neointimal hyperplasia in balloon-injured (BI) rat carotid artery models through downregulation of the chemokine and adhesion molecules by inhibiting nuclear factor (NF)-κB activity.[25,26] However, the potential proapoptotic effect of ALA on VSMCs and its role in postinjury reendothelialization and platelet aggregation have not yet been explored.

In this study, we investigated whether ALA inhibits neointimal hyperplasia via induction of VSMC apoptosis and identified the signaling pathways involved in this process. Also, we examined the potential effect of ALA on postinjury reendothelialization and platelet aggregation.

Methods

Male Sprague-Dawley rats (Hyochang, Daegu, Korea), aged 7 to 8 weeks and weighing 280 to 300 g, were used in the experiments. All procedures complied with the institutional guidelines for animal research.

An expanded Methods section is available in the supplemental data (available online at http://atvb.ahajournals.org).

Results

ALA Induces Apoptosis of VSMCs

Based on our observation of a dramatic decrease in the number of VSMCs by ALA treatment (data not shown), we investigated the effect of ALA on VSMC proliferation and apoptosis through cell cycle analysis using flow cytometry. ALA treatment for 22 hours suppressed cell cycle progression from G_0/G_1 to S phase in serum-stimulated VSMCs (supplemental Figure I). When VSMCs were incubated in complete medium containing 10% FBS and ALA for 72 hours, the percentage of cells in the sub-G_1 phase, indicative of an apoptotic population, was greatly enriched (Figure 1A). In contrast, the sub-G_1 population was modestly increased in quiescent VSMCs, which were incubated in medium with 0.5% FBS and ALA (supplemental Figure II). This result suggests that ALA induces apoptosis more potently in proliferating than quiescent VSMCs. This proapoptotic effect of ALA on VSMCs was further confirmed by TUNEL staining (Figure 1B).

In addition, ALA significantly increased the expression of a proapoptotic molecule, BCL2-associated X protein (Bax), and subsequent cytosolic release of cytochrome C from mitochondria (Figure 1C). ALA also strongly activated caspase-3, a key executioner of apoptosis, as determined by amino acid sequence Asp-Glu-Val-Asp (DEVD)ase activity (Figure 1D). These results demonstrate that ALA induces apoptosis of VSMCs through an intrinsic mitochondria-mediated apoptotic pathway.

ALA Enhances Expression and Cytoplasmic Localization of Nur77 in VSMCs

Nur77 is induced in response to various apoptotic stimuli and is involved in the intrinsic apoptotic pathway in cancer cell lines.[13–17] Thus, we examined the effect of ALA on Nur77 expression in VSMCs. Replacement with complete medium without ALA resulted in a rapid and transient induction of Nur77 mRNA that increased at 30 minutes to 2 hours but returned to baseline levels by 4 hours (Figure 2A, left). In contrast, Nur77 mRNA expression was slightly enhanced by ALA at 2 hours and significantly induced at 8 to 24 hours, suggesting biphasic induction of Nur77 by ALA. In addition, a transient transfection assay showed that ALA increased Nur77 promoter activity, suggesting that ALA regulates Nur77 expression at a transcriptional level (Figure 2A, right).

Immunocytochemical staining revealed that complete medium alone transiently increased nuclear Nur77 protein expression, whereas ALA-containing complete medium further enhanced cytoplasmic and nuclear Nur77 expression at 2 hours (Figure 2B). Cytoplasmic Nur77 expression persisted up to 12 hours, although the signal was weak, whereas it was rarely detected in ALA-untreated VSMCs. Moreover, similar to other apoptotic stimuli,[12] ALA repressed transcriptional activity of Nur77 (supplemental Figure III), implying that the nuclear transactivation function of Nur77 is dispensable for the proapoptotic effect of ALA.

Immunofluorescence analysis also showed that a significant amount of Nur77 was diffusely distributed throughout the cytoplasm in ALA-treated, but not untreated, VSMCs (Figure 2C). ALA induced cytoplasmic localization of some fraction of Nur77 protein, noticeably in mitochondria, as evidenced by partial coimmunostaining with heat shock protein 60, a mitochondria-specific protein.[16] Moreover, Nur77 interacted with Bcl-2 in the presence of ALA (Figure 2D), implying that ALA-induced VSMC apoptosis can be mediated by the interaction of Nur77 with Bcl-2, similar to previous reports.[16,17] Altogether, these findings demonstrate that ALA enhances the

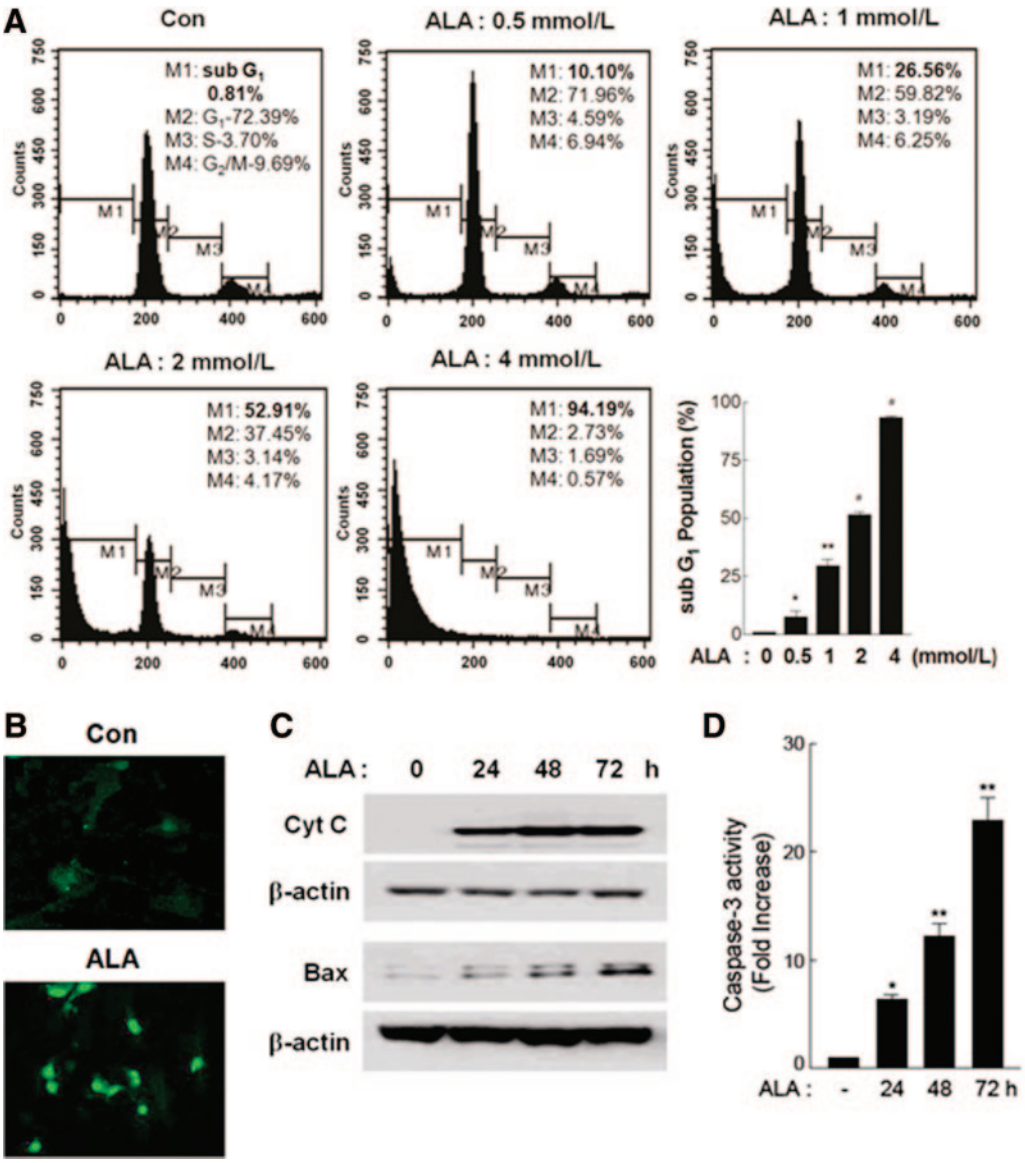

Figure 1. ALA induces VSMC apoptosis via an intrinsic mitochondrial pathway. A, Flow cytometry analysis. VSMCs were treated with complete medium containing indicated concentrations of ALA for 72 hours, stained with propidium iodide (PI), and analyzed by flow cytometry. The M_1 (sub-G_1) cell population represents apoptotic cells. Data in the bar graph are the mean±SE of 3 independent measurements. $^{*}P<0.01$, $^{**}P<0.005$, and $^{\#}P<0.001$ vs control. B, VSMCs were treated with ALA, 2 mmol/L, for 24 hours; and apoptotic nuclei (green) were detected by TUNEL staining. C, Cytosolic proteins and whole cell lysates were analyzed by Western blotting using anti–cytochrome C (Cyt C) antibody and anti–Bax antibody, respectively. D, The activity of the caspase-3–like enzyme (DEVDase) was measured by monitoring release of chromophore p-nitroanilide. $^{*}P<0.01$ and $^{**}P<0.005$ vs control at 72 hours. Con indicates control.

expression and nuclear export of Nur77, and interaction between Nur77 and Bcl-2, leading to subsequent VSMC apoptosis.

Nur77 Is Required for ALA-Induced VSMC Apoptosis

To verify the requirement of Nur77 for ALA-induced VSMC apoptosis, we examined the effect of knockdown of Nur77. ALA-induced Nur77 expression was profoundly reduced by transient transfection of small interfering RNA (siRNA) targeting Nur77 (Nur77-siRNA) but not control siRNA (Con-siRNA) (Figure 3A). The percentage of ALA-increased apoptotic cells was evidently reduced by Nur77-siRNA, indicating that Nur77 is indispensable for ALA-induced VSMC apoptosis (Figure 3B and C). Similarly, ALA-induced caspase-3 activity was significantly diminished by Nur77-siRNA (Figure 3D). Taken together, these results reveal that Nur77 is required for ALA-induced apoptosis of VSMCs.

p38 Mitogen-Activated Protein Kinase Plays a Critical Role in ALA-Induced VSMC Apoptosis Through Modulation of Expression and Cytoplasmic Localization of Nur77

To clarify the signal transduction pathways involved in ALA-induced Nur77 expression and apoptosis, we examined the effect of inhibitors of diverse signaling pathways, including mitogen-activated protein kinases (MAPKs) (ie, extracellular signal–regulated kinase [ERK], JNK, and p38 MAPK), protein kinase A, protein kinase C, and phosphatidylinositol

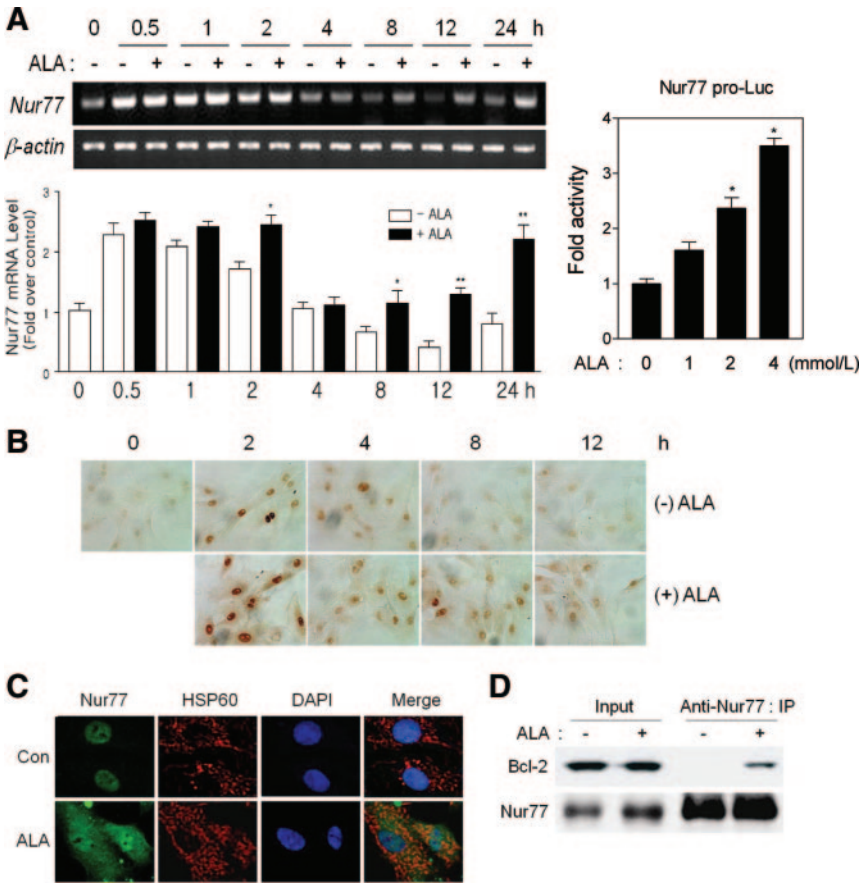

Figure 2. ALA enhances the expression and cytoplasmic localization of Nur77. A, ALA increased Nur77 expression at a transcriptional level. At 24 hours after seeding of VSMCs, medium was replaced with fresh complete medium containing ALA. Cells were then incubated for indicated times and harvested for semiquantitative RT-PCR (left). Levels of Nur77 mRNA were normalized against those of β-actin, and data in the bar graph are the mean±SE of 3 independent measurements. *$P<0.05$ and **$P<0.01$ vs control. Transient transfection assay results are also given (right). VSMCs were transfected with Nur77 pro-Luc and treated with ALA for 24 hours. Luciferase activity was normalized to β-galactosidase activity. *$P<0.05$ vs reporter alone. B, Immunocytochemical staining for Nur77 in VSMCs treated with ALA, 2 mmol/L. C, Subcellular localization of Nur77 was detected by immunofluorescence. VSMCs were treated with ALA for 2 hours and immunostained with anti-Nur77 and anti–heat shock protein (HSP) 60 antibodies. Cells were stained with 4′,6-diamidino-2-phenylindole (DAPI) to identify nuclei. Nur77, HSP60 (mitochondria), and DAPI (nuclei) were visualized by confocal microscopy; and the images were overlaid. D, ALA stimulates the interaction between Nur77 and Bcl-2. VSMCs were treated with ALA, cell lysates were immunoprecipitated using anti–Nur77 antibody, and the immune complex was subjected to Western blotting with anti–Bcl-2 antibody. Con indicates control; Nur77 pro-Luc, Nur77 promoter-driven luciferase reporter.

3-kinase. Among the inhibitors tested, only SB203580, a selective inhibitor of p38 MAPK, completely blocked ALA-induced Nur77 mRNA expression and morphological changes in VSMCs; although GF109203X, a protein kinase C inhibitor, also showed a modest effect (Figure 4A). In contrast, inhibition of ERK, JNK, protein kinase A, and phosphatidylinositol 3-kinase further enhanced Nur77 expression and could not reverse the morphological changes of VSMCs evoked by ALA.

As expected, ALA increased p38 MAPK phosphorylation from 30 minutes up to 8 hours, whereas it moderately inhibited JNK and ERK1/2 phosphorylation (Figure 4B). ALA-induced increases in the sub-G_1 cell population and caspase-3 activity were markedly suppressed by SB203580 but not by an ERK inhibitor, PD98059 (Figure 4C). Moreover, ALA-induced cytoplasmic localization of Nur77 was extensively reduced by SB203580 (Figure 4D). Collectively, these findings demonstrate that ALA induces apoptosis of VSMCs through p38 MAPK-dependent induction and cytoplasmic localization of Nur77.

ALA Prevents Neointimal Hyperplasia Via Induction of Nur77-Mediated VSMC Apoptosis

To validate the proapoptotic effect of ALA on VSMCs in vivo, we used a rat carotid artery BI model; and TUNEL staining was performed on the sections of arteries of rats intraperitoneally administered saline (vehicle) or ALA from 3 day before to 14 days after BI. ALA administration significantly reduced neointimal hyperplasia in the vessels at 14 days after BI (Figure 5A and supplemental Figure IV). There were few apoptotic cells in uninjured control arteries, irrespective of ALA treatment (Figure 5B, left), indicating no toxic effect of ALA on healthy arteries. In contrast, TUNEL-positive cells were greatly increased in injured arteries of rats given ALA. Similar results were obtained by transmission electron microscopy (supplemental Figure V). Moreover, apoptotic cells were detected predominantly in the neointima of ALA-treated arteries, where VSMCs actively proliferate, compared with those in the media. This result was consistent with the observation that proliferating neointimal VSMCs were more sensitive to the proapoptotic effect of ALA versus quiescent medial VSMCs (Figure 5C).

In agreement with TUNEL staining, strong cytoplasmic Nur77 expression was observed, especially in the neointima of ALA-treated arteries at 14 days after BI; whereas it was barely detected in either media or neointima of saline-treated arteries (Figure 5B, right). To confirm the requirement of Nur77 for a protective effect of ALA against neointimal hyperplasia, we infused adenoviruses encoding shRNA against Nur77 or control shRNA in BI carotid arteries. Adenoviruses encoding shRNA against Nur77, but not adenoviruses encoding control shRNA, significantly reduced the inhibitory effect of ALA on neointima formation (Figure 5D and supplemental Figure VI). This finding demonstrates a requirement of Nur77 for ALA-induced protection against neointimal hyperplasia. Altogether, these results demonstrate that ALA prevents neointimal hyperplasia after vascular

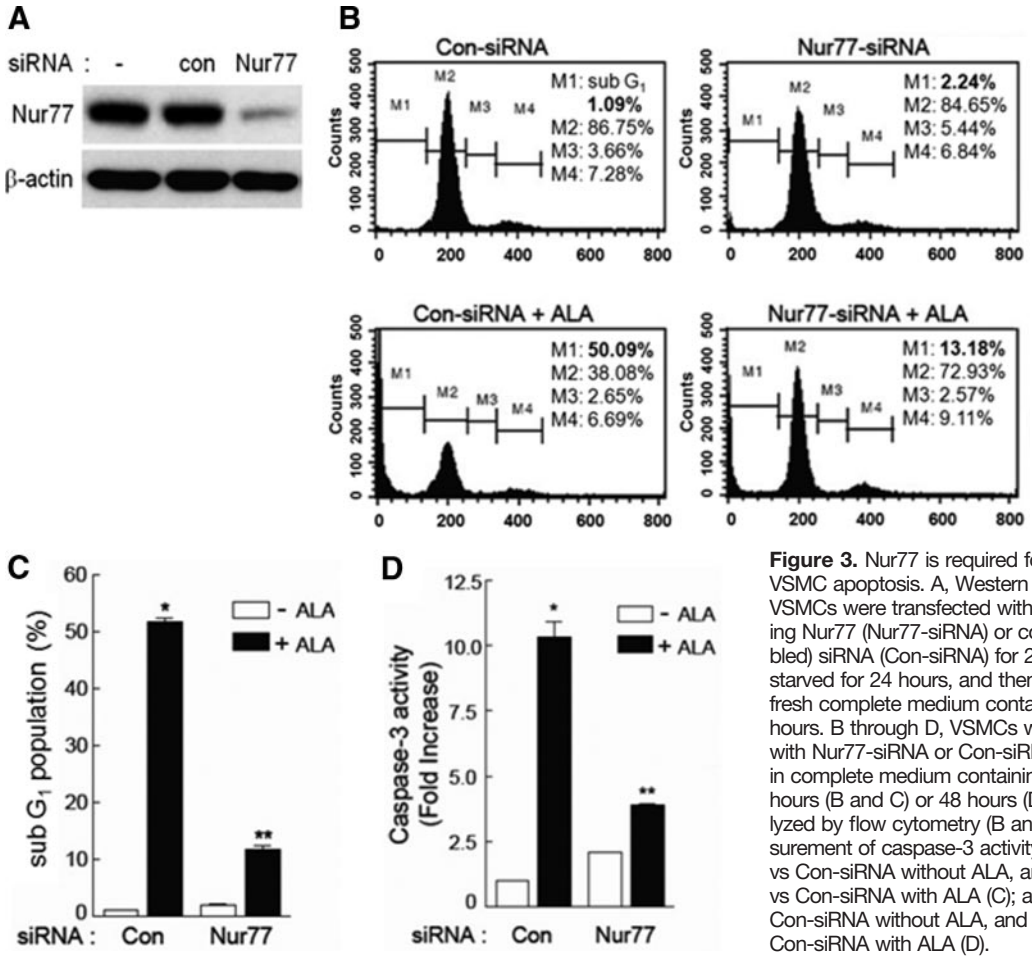

Figure 3. Nur77 is required for ALA-induced VSMC apoptosis. A, Western blot analysis. VSMCs were transfected with siRNA, targeting Nur77 (Nur77-siRNA) or control (scrambled) siRNA (Con-siRNA) for 24 hours, serum starved for 24 hours, and then incubated in fresh complete medium containing ALA for 2 hours. B through D, VSMCs were transfected with Nur77-siRNA or Con-siRNA, incubated in complete medium containing ALA for 72 hours (B and C) or 48 hours (D), and analyzed by flow cytometry (B and C) or measurement of caspase-3 activity (D). *$P<0.005$ vs Con-siRNA without ALA, and **$P<0.01$ vs Con-siRNA with ALA (C); and *$P<0.01$ vs Con-siRNA without ALA, and **$P<0.05$ vs Con-siRNA with ALA (D).

injury, at least partly through induction of Nur77-mediated apoptosis in VSMCs.

ALA Accelerates Reendothelialization After BI and Inhibits Platelet Aggregation

Incomplete or delayed reendothelialization, leading to LST, remains a major problem of DESs; and accelerated reendothelialization has reduced restenosis and LST.[3,7–9] Based on previous studies[24,27] showing protective effects of ALA on endothelial cells, we examined the effect of ALA on reendothelialization by immunohistochemical staining for CD31, an endothelial-specific marker, on the sections of arteries harvested at various points (3, 10, and 14 days after injury). ALA significantly increased CD31 reactivity on the luminal surface of arteries at 10 to 14 days after injury, whereas a CD31 signal was undetectable in injured arteries without ALA administration (Figure 6A).

In contrast with its proapoptotic action in VSMCs, ALA did not induce apoptosis of human aortic endothelial cells (HAECs); rather, it inhibited basal apoptosis of HAECs (Figure 6B) whereas it inhibited proliferation of HAECs (Figure 6C). Moreover, ALA strongly inhibited arachidonic acid–induced platelet aggregation, suggesting its antithrombotic property (Figure 6D). Taken together, these results propose that ALA may prevent restenosis and LST after DES implantation through facilitation of reendothelialization and direct inhibition of platelet aggregation.

Discussion

In this study, we demonstrate that ALA inhibits neointima formation in BI rat carotid arteries by inducing apoptosis of VSMCs. We also elucidated the detailed molecular mechanisms underlying ALA-induced VSMC apoptosis, which was associated with the p38 MAPK/Nur77-mediated apoptotic pathway. In contrast, ALA inhibited basal apoptosis of endothelial cells and accelerated reendothelialization after BI. We also found an antiplatelet aggregation effect of ALA. Therefore, our findings suggest that ALA may prevent restenosis and LST after DES implantation through induction of VSMC apoptosis and acceleration of reendothelialization, along with its direct antithrombotic effect.

ALA has induced or inhibited apoptosis, depending on the cell types and cellular context.[20,22,24] However, the detailed mechanisms of its conflicting actions in relation to apoptosis have not been fully investigated. Previously, ALA prevented apoptosis of endothelial cells via AMP-activated protein kinase phosphorylation and antioxidative function.[24] Herein, we demonstrated differential effects on apoptosis of VSMCs and endothelial cells. We elucidated the molecular mechanism underlying proapoptotic action of ALA on VSMCs, involving p38 MAPK–dependent Nur77 induction and cytoplasmic localization. In contrary, ALA inhibited basal apoptosis of HAECs, even at a high concentration (4 mmol/L), and accelerated reendothelialization in vivo. This antiapoptot-

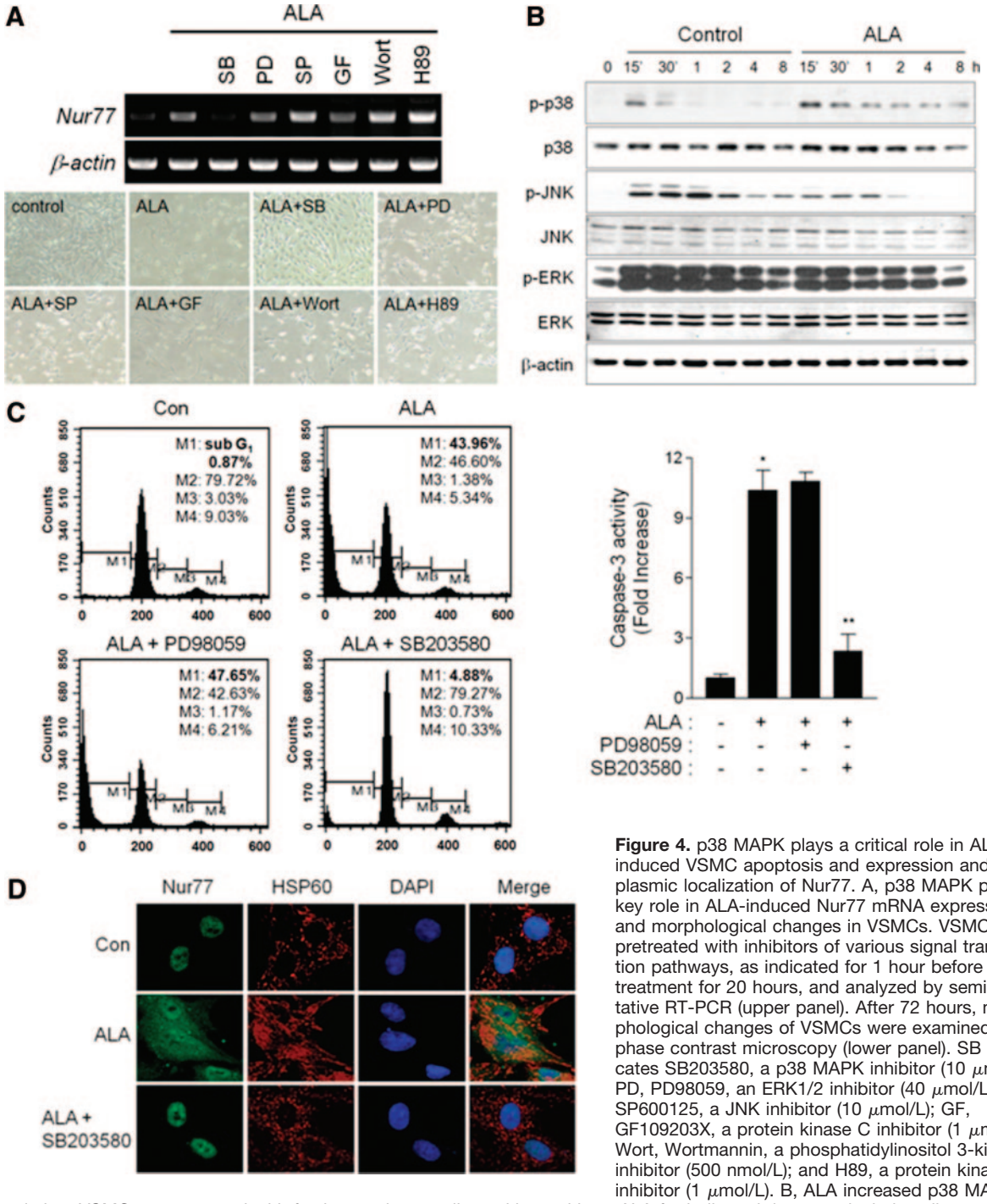

Figure 4. p38 MAPK plays a critical role in ALA-induced VSMC apoptosis and expression and cytoplasmic localization of Nur77. A, p38 MAPK plays a key role in ALA-induced Nur77 mRNA expression and morphological changes in VSMCs. VSMCs were pretreated with inhibitors of various signal transduction pathways, as indicated for 1 hour before ALA treatment for 20 hours, and analyzed by semiquantitative RT-PCR (upper panel). After 72 hours, morphological changes of VSMCs were examined by phase contrast microscopy (lower panel). SB indicates SB203580, a p38 MAPK inhibitor (10 μmol/L); PD, PD98059, an ERK1/2 inhibitor (40 μmol/L); SP, SP600125, a JNK inhibitor (10 μmol/L); GF, GF109203X, a protein kinase C inhibitor (1 μmol/L); Wort, Wortmannin, a phosphatidylinositol 3-kinase inhibitor (500 nmol/L); and H89, a protein kinase A inhibitor (1 μmol/L). B, ALA increased p38 MAPK phosphorylation. VSMCs were treated with fresh complete medium with or without ALA for indicated times, and whole cell extracts were subjected to Western blotting. C, Inhibition of p38 MAPK blocked ALA-induced VSMC apoptosis. VSMCs were pretreated with SB203580 or PD98059 for 1 hour before ALA treatment for 72 hours and analyzed by flow cytometry and measurement of caspase-3 activity. *$P<0.01$ vs control at 48 hours, and **$P<0.01$ vs ALA alone. D, Cells were treated with SB203580 for 1 hour before ALA treatment for 2 hours and fixed for immunostaining with anti–Nur77 and anti–heat shock protein (HSP) 60 antibodies. DAPI indicates 4′,6-diamidino-2-phenylindole; p, phosphorylated.

ic action of ALA might be mediated through activation of AMP-activated protein kinase or acutely transforming retrovirus AKT8 in rodent T cell lymphoma (AKT), as suggested in previous studies.[24,27] Further studies are necessary to elucidate the molecular mechanism of antiapoptotic action of ALA in HAECs.

Recently, Nur77 family members have emerged as potentially important factors in the complex network of proteins that modulate endothelial cell activation and VSMC proliferation in atherosclerosis.[10,28–30] Overexpression of TR3 in the arterial VSMCs and activation of Nur77 by 6-mercaptopurine protect against neointimal formation through inhibition of

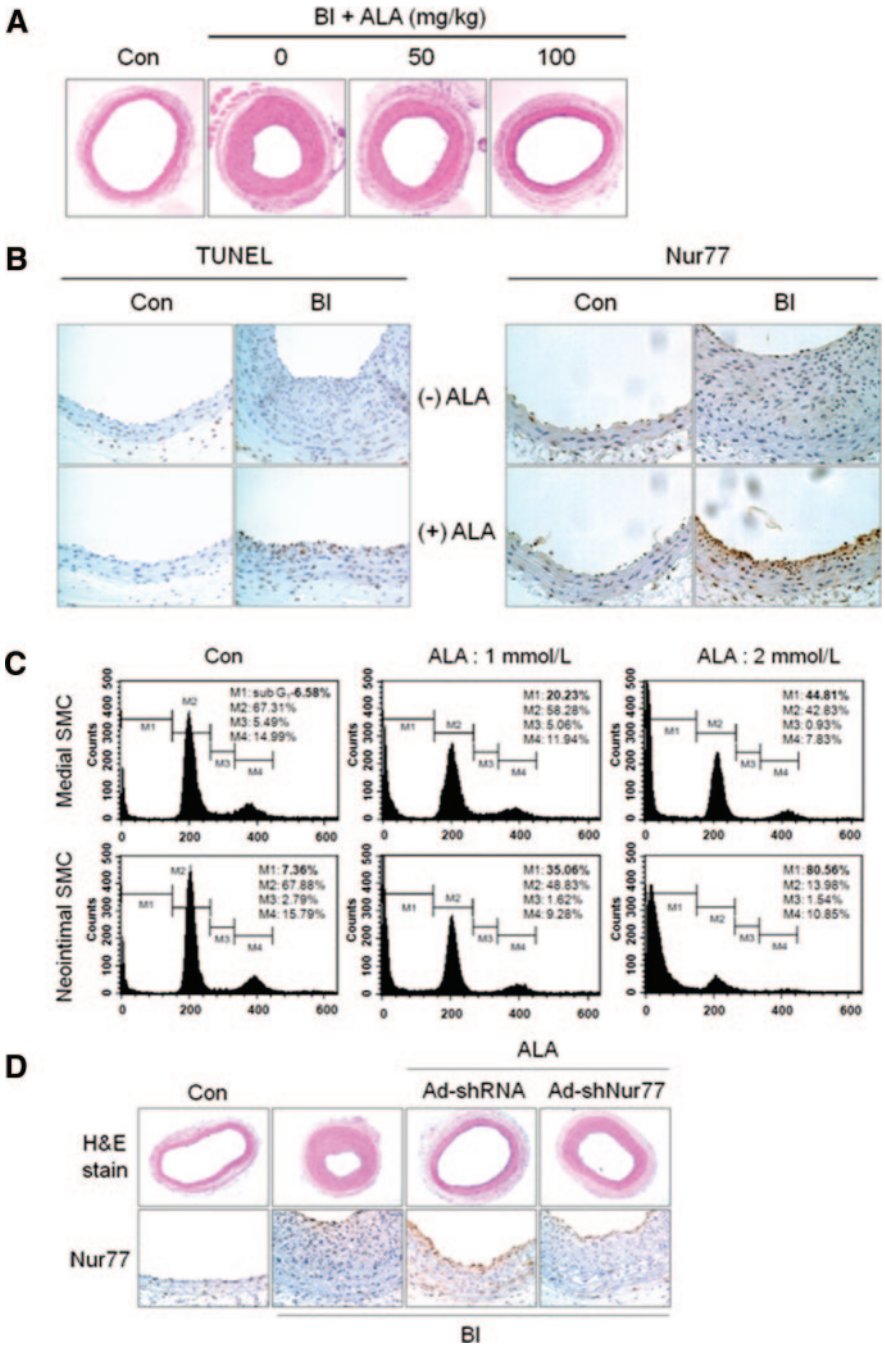

Figure 5. ALA prevents neointimal hyperplasia via induction of Nur77-mediated VSMC apoptosis. A, Representative photomicrographs of cross-sections of uninjured (con) and BI carotid arteries of rats given saline or ALA, 50 and 100 mg/kg per day, from 3 days before to 14 days after BI (hematoxylin-eosin [H&E] stain, original magnification ×100). B, TUNEL staining (left) and immunohistochemical staining (right) for Nur77 were performed on the cross-sections (hematoxylin stain, original magnification ×200). C, Neointimal VSMCs are more sensitive to ALA-induced apoptosis than medial VSMCs. Neointimal and medial VSMCs were incubated with ALA, 1 and 2 mmol/L, for 72 hours and analyzed by flow cytometry. D, Adenoviruses encoding shRNA against Nur77 (Ad-shNur77) markedly diminished the inhibitory effect of ALA on neointimal hyperplasia. Ad-shNur77 or adenoviruses encoding control shRNA (Ad-shRNA) were infused into BI carotid arteries of rats immediately after injury, and rats were given ALA from 3 days before to 14 days after BI (H&E stain, original magnification ×100). Immunohistochemical staining for Nur77 (brown) was performed (hematoxylin stain, original magnification ×200).

excessive VSMC proliferation via induction of cell cycle arrest but not apoptosis.[18,19] Herein, we suggest an alternative inhibitory mechanism of neointimal hyperplasia by ALA through induction of p38 MAPK/Nur77-mediated apoptosis of VSMCs. ALA-induced VSMC apoptosis and protection against neointimal hyperplasia were significantly abrogated by downregulation of Nur77. It was previously reported that ALA inhibited vascular inflammation by inhibiting the NF-κB pathway, leading to the inhibition of neointimal hyperplasia.[24–26] Considering the previous reports[28–30] that Nur77 inhibits NF-κB activity, it is also plausible that the anti-inflammatory effect of ALA may be mediated, at least in part, by Nur77. In support of this theory, we found that Nur77 siRNA significantly reduced the inhibitory effect of ALA on TNF-α–stimulated NF-κB activity (supplemental Figure VII). Therefore, ALA may exert antirestenotic effects primarily through Nur77 because ALA-induced Nur77 could mediate the anti-inflammatory action of ALA in injured vessels and because of its proapoptotic effect on proliferating VSMCs. However, further studies are needed to confirm the hypothesis in vivo and to identify the transcription factors mediating ALA responsiveness on the *Nur77* gene promoter.

Recent advances in DESs, such as sirolimus- or paclitaxel-eluting stents, have significantly reduced the incidence of in-stent restenosis. However, the risk of LST remains a severe complication after DES implantation and is caused, in part, by delayed or incomplete reendothelialization because of its

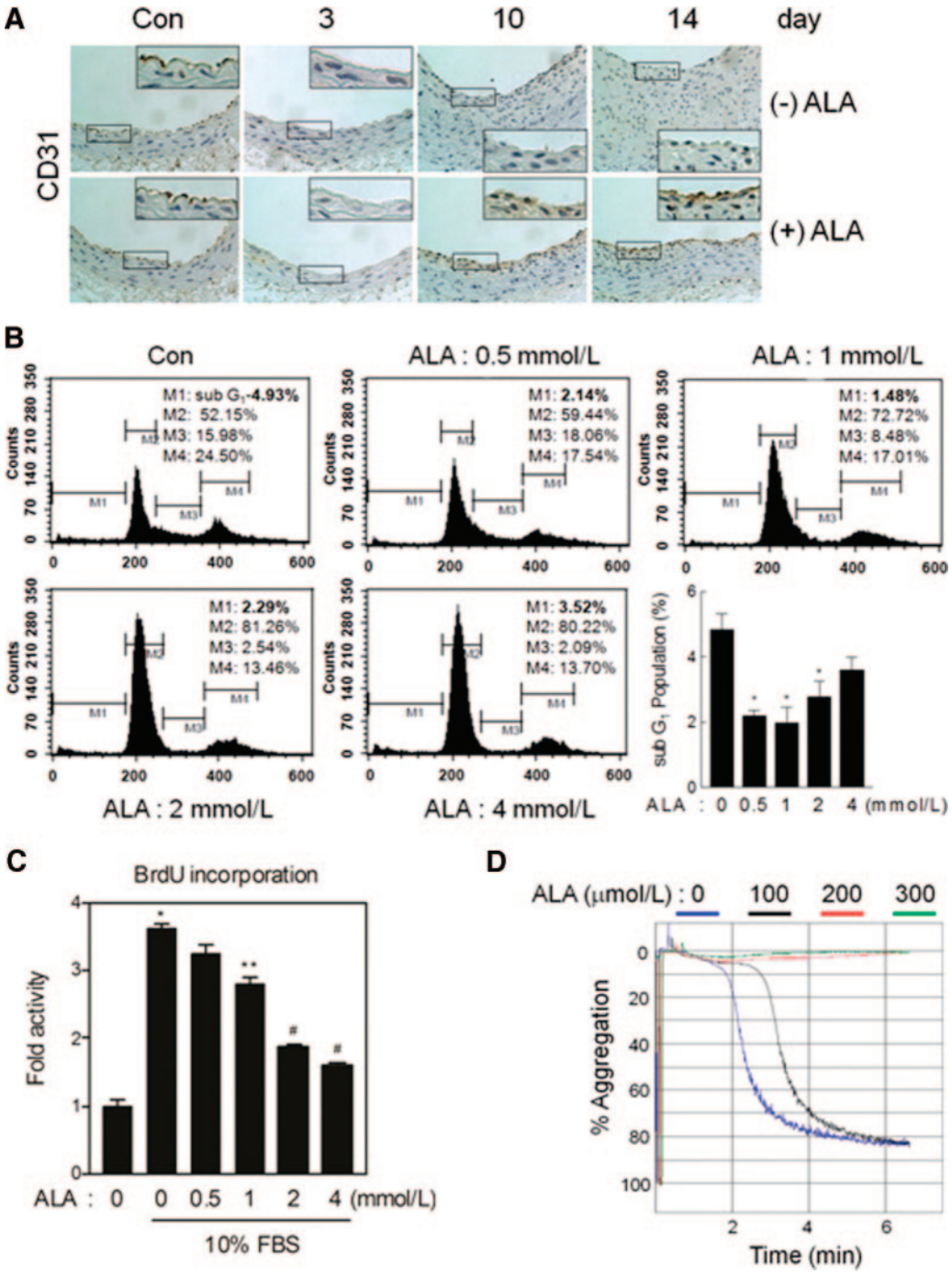

Figure 6. ALA accelerates postinjury reendothelialization and inhibits platelet aggregation. A, Immunohistochemical staining for CD31 (brown), an endothelial-specific marker, was performed on the cross-sections of control arteries and the arteries of rats administered saline or ALA, 100 mg/kg per day, and harvested at 3, 10, and 14 days after BI (hematoxylin stain, original magnification ×200). B, ALA inhibits basal apoptosis of HAECs. HAECs were treated with ALA for 72 hours and analyzed by flow cytometry. C, ALA inhibited proliferation of HAECs. Serum-starved HAECs with 0.5% FBS for 24 hours were stimulated with 10% FBS and ALA for 16 hours and incubated with 5-bromodeoxyuridine (BrdU) for an additional 2 hours. *$P<0.001$ vs control, and **$P<0.01$ and $^{\#}P<0.001$ vs serum-stimulated activity. D, ALA inhibits arachidonic acid (AA)–induced human platelet aggregation. Human platelets were incubated with ALA and stimulated with AA, 1 mmol/L.

cytotoxic effects on endothelial cells and VSMCs and vascular inflammation.[3,7–9] Therefore, successful development of a DES has relied on discovery of agents that play opposite actions in VSMCs and endothelial cells in terms of proliferation and apoptosis. In addition, antiplatelet therapy is mandatory to prevent LST after DES implantation, although there is still a debate about the optimal duration of antiplatelet therapy.[3,7,31] Herein, we demonstrated that ALA prevented HAEC apoptosis and accelerated postinjury reendothelialization in vivo. We also showed an antiplatelet aggregation property of ALA, suggesting its direct antithrombotic effect. Collectively, our previous and present studies suggest that

ALA can be a promising therapeutic agent used in DESs for the prevention of restenosis and LST after DES implantation because of its pleiotropic effects on diverse vascular and inflammatory cells.

Acknowledgments

ALA was kindly donated by Viatris GmbH & Co KG, Frankfurt, Germany.

Sources of Funding

This study was supported by a Future-Based Technology Development Program (BIO Fields, 2010-0019511) and a World Class University Program (R32-10064) through the National Research Foundation of Korea; Science Research Center grant to Bone Metabolism Research Center (2010-0001742); National Research Foundation grants 2010-0019511, R32-10064, 2010-0001742, 2010-0020532, and 2010-0008023, funded by the Korean Ministry of Education, Science and Technology; a grant from the Korean Ministry of Education, Science and Technology (The Regional Core Research Program/Anti-aging and Well-being Research Center); and the Brain Korea 21 project in 2010.

Disclosures

None.

References

1. Dzau VJ, Braun-Dullaeus RC, Sedding DG. Vascular proliferation and atherosclerosis: new perspectives and therapeutic strategies. *Nat Med*. 2002;8:1249–1256.
2. Schwartz SM, deBlois D, O'Brien ER. The intima: soil for atherosclerosis and restenosis. *Circ Res*. 1995;77:445–465.
3. Costa MA, Simon DI. Molecular basis of restenosis and drug-eluting stents. *Circulation*. 2005;111:2257–2273.
4. Ruiz E, Gordillo-Moscoso A, Padilla E, Redondo S, Rodriguez E, Reguillo F, Briones AM, van Breemen C, Okon E, Tejerina T. Human vascular smooth muscle cells from diabetic patients are resistant to induced apoptosis due to high Bcl-2 expression. *Diabetes*. 2006;55:1243–1251.
5. Suzuki J, Isobe M, Morishita R, Nishikawa T, Amano J, Kaneda Y. Antisense Bcl-x oligonucleotide induces apoptosis and prevents arterial neointimal formation in murine cardiac allografts. *Cardiovasc Res*. 2000;45:783–787.
6. Pollman MJ, Hall JL, Mann MJ, Zhang L, Gibbons GH. Inhibition of neointimal cell bcl-x expression induces apoptosis and regression of vascular disease. *Nat Med*. 1998;4:222–227.
7. Joner M, Finn AV, Farb A, Mont EK, Kolodgie FD, Ladich E, Kutys R, Skorija K, Gold HK, Virmani R. Pathology of drug-eluting stents in humans: delayed healing and late thrombotic risk. *J Am Coll Cardiol*. 2006;48:193–202.
8. Hutter R, Sauter BV, Reis ED, Roque M, Vorchheimer D, Carrick FE, Fallon JT, Fuster V, Badimon JJ. Decreased reendothelialization and increased neointima formation with endostatin overexpression in a mouse model of arterial injury. *Circulation*. 2003;107:1658–1663.
9. Asahara T, Bauters C, Pastore CJ, Kearney M, Rossow S, Bunting S, Ferrara N, Symes JF, Isner JM. Local delivery of vascular endothelial growth factor accelerates reendothelialization and attenuates intimal hyperplasia in balloon-injured rat carotid artery. *Circulation*. 1995;91:2793–2801.
10. Martínez-González J, Badimon L. The NR4A subfamily of nuclear receptors: new early genes regulated by growth factors in vascular cells. *Cardiovasc Res*. 2005;65:609–618.
11. Williams GT, Lau LF. Activation of the inducible orphan receptor gene Nur77 by serum growth factors: dissociation of immediate early and delayed-early responses. *Mol Cell Biol*. 1993;13:6124–6136.
12. Fahrner TJ, Carroll SL, Milbrandt J. The NGFI-B protein, an inducible member of the thyroid/steroid receptor family, is rapidly modified post-translationally. *Mol Cell Biol*. 1990;10:6454–6459.
13. Liu ZG, Smith SW, McLaughlin KA, Schwartz LM, Osborne BA. Apoptotic signals delivered through the T-cell receptor of a T-cell hybrid require the immediate-early gene nur77. *Nature*. 1994;367:281–284.
14. Woronicz JD, Calnan B, Ngo V, Winoto A. Requirement for the orphan steroid receptor Nur77 in apoptosis of T-cell hybridomas. *Nature*. 1994;367:277–281.
15. Andrew JW, Diego A, John MM, Barbara GH, Leonard HA. TR3/Nur77 in colon cancer cell apoptosis. *Cancer Res*. 2003;63:5401–5407.
16. Li H, Kolluri SK, Gu J, Dawson MI, Cao X, Hobbs PD, Lin B, Chen G, Lu J, Lin F, Xie Z, Fontana JA, Reed JC, Zhang XK. Cytochrome c release and apoptosis induced by mitochondrial targeting of nuclear orphan receptor TR3. *Science*. 2000;289:1159–1164.
17. Lin B, Kolluri SK, Lin F, Liu W, Han YH, Cao X, Dawson MI, Reed JC, Zhang XK. Conversion of Bcl-2 from protector to killer by interaction with nuclear orphan receptor Nur77/TR3. *Cell*. 2004;116:527–540.
18. Arkenbout EK, de Waard V, van Bragt M, van Achterberg TA, Grimbergen JM, Pichon B, Pannekoek H, de Vries CJ. Protective function of transcription factor TR3 orphan receptor in atherogenesis: decreased lesion formation in carotid artery ligation model in TR3 transgenic mice. *Circulation*. 2002;106:1530–1535.
19. Pires NM, Pols TW, de Vries MR, van Tiel CM, Bonta PI, Vos M, Arkenbout EK, Pannekoek H, Jukema JW, Quax PH, de Vries CJ. Activation of nuclear receptor Nur77 by 6-mercaptopurine protects against neointima formation. *Circulation*. 2007;115:493–500.
20. Novotny L, Rauko P, Cojocel C. alpha-Lipoic acid: the potential for use in cancer therapy. *Neoplasma*. 2008;55:81–86.
21. Shay KP, Moreau RF, Smith EJ, Smith AR, Hagen TM. Alpha-lipoic acid as a dietary supplement: molecular mechanisms and therapeutic potential. *Biochim Biophys Acta*. 2009;1790:1149–1160.
22. Van de Mark K, Chen JS, Steliou K, Perrine SP, Faller DV. a-Lipoic acid induces $p27^{Kip}$-dependent cell cycle arrest in non-transformed cell lines and apoptosis in tumor cell lines. *J Cell Physiol*. 2004;194:325–340.
23. Yi X, Maeda N. Alpha-lipoic acid prevents the increase in atherosclerosis induced by diabetes in apolipoprotein E-deficient mice fed high-fat/low-cholesterol diet. *Diabetes*. 2006;55:2238–2244.
24. Lee WJ, Lee IK, Kim HS, Kim YM, Koh EH, Won JC, Han SM, Kim MS, Jo IH, Oh GT, Par IS, Youn JH, Park SW, Lee KU, Park JY. Alpha-lipoic acid prevents endothelial dysfunction in obese rats via activation of AMP-activated protein kinase. *Arterioscler Thromb Vasc Biol*. 2005;25:2488–2494.
25. Lee KM, Park KG, Kim YD, Lee HJ, Kim HT, Cho WH, Kim HS, Han SW, Koh GY, Park JY, Lee KU, Kim JG, Lee IK. Alpha-lipoic acid inhibits fractalkine expression and prevents neointimal hyperplasia after balloon injury in rat carotid artery. *Atherosclerosis*. 2006;189:106–114.
26. Kim HS, Kim HJ, Park KG, Kim YN, Kwon TK, Park JY, Lee KU, Park JG, Lee IK. α-Lipoic acid inhibits matrix metalloproteinase-9 expression by inhibiting NF-κB transcriptional activity. *Exp Mol Med*. 2007;39:106–113.
27. Artwohl M, Muth K, Kosulin K, de Martin R, Hölzenbein T, Rainer G, Freudenthaler A, Huttary N, Schmetterer L, Waldhäusl WK, Baumgartner-Parzer SM. R-(+)-alpha-lipoic acid inhibits endothelial cell apoptosis and proliferation: involvement of Akt and retinoblastoma protein/E2F-1. *Am J Physiol Endocrinol Metab*. 2007;293:E681–E689.
28. Pols TW, Bonta PI, de Vries CJ. NR4A nuclear orphan receptors: protective in vascular disease? *Curr Opin Lipidol*. 2007;18:515–520.
29. You B, Jiang YY, Chen S, Yan G, Sun J. The orphan nuclear receptor Nur77 suppresses endothelial cell activation through induction of IkappaBalpha expression. *Circ Res*. 2009;104:742–749.
30. Evans PC. Nur77: orphaned at birth but adopted by the nuclear factor kappaB signaling pathway. *Circ Res*. 2009;104:707–709.
31. Austin D, Pell JP, Oldroyd KG. Drug-eluting stents: a review of current evidence on clinical effectiveness and late complications. *Scott Med J*. 2008;53:16–24.

Arteriosclerosis, Thrombosis, and Vascular Biology

JOURNAL OF THE AMERICAN HEART ASSOCIATION

α-Lipoic Acid Prevents Neointimal Hyperplasia Via Induction of p38 Mitogen-Activated Protein Kinase/Nur77-Mediated Apoptosis of Vascular Smooth Muscle Cells and Accelerates Postinjury Reendothelialization

Han-Jong Kim, Joon-Young Kim, Sun Joo Lee, Hye-Jin Kim, Chang Joo Oh, Young-Keun Choi, Hyo-Jeong Lee, Ji-Yeon Do, Sun-Yee Kim, Taeg-Kyu Kwon, Hueng-Sik Choi, Mi-Ock Lee, In-Sun Park, Keun-Gyu Park, Ki-Up Lee and In-Kyu Lee

Arterioscler Thromb Vasc Biol. 2010;30:2164-2172; originally published online September 9, 2010;
doi: 10.1161/ATVBAHA.110.212308
Arteriosclerosis, Thrombosis, and Vascular Biology is published by the American Heart Association, 7272 Greenville Avenue, Dallas, TX 75231

Print ISSN: 1079-5642. Online ISSN: 1524-4636

Supplemental Materials

Materials and Methods

Cell Culture

VSMCs were isolated from the thoracic aorta of 4-week-old male SD rats using the explant method (1) and cultured in Dulbecco's Modified Eagle Medium (DMEM; Invitrogen, Carlsbad, CA) supplemented with 20% fetal bovine serum (FBS; Thermo Scientific HyClone, Logan, UT) and antibiotics. VSMC purity was determined by positive staining with smooth-muscle-specific α-actin monoclonal antibody (Sigma, St. Louis, MO). VSMCs were maintained in complete medium (DMEM supplemented with 10% FBS) and cells from the fourth to seventh passages were used for all the experiments. Neointimal and medial SMCs were isolated from the balloon-injured and uninjured carotid arteries by enzyme digestion method as described previously (2) and cultured in DMEM supplemented with 20% FBS and antibiotics. Isolated neointimal and medial SMCs were used passages between 2 and 3. Human aortic endothelial cells (HAECs, Clonetics Corporation, San Diego, CA) were cultured in EGM-2 growth medium supplemented with 2% FBS and used passages between 5 and 7. HepG2 cells were cultured in MEM supplemented with 10% FBS and antibiotics.

Flow cytometric analysis

To examine the effect of ALA on the cell cycle distribution, VSMCs (1.4×10^4 cells/cm^2, unless otherwise stated) were serum starved for 48 h and stimulated with 20% FBS in the presence of ALA (0, 0.5, 1, 2 and 4 mmol/L) for 22 h. To detect the apoptosis, VSMCs, intimal and medial VSMCs isolated from carotid arteries 14 days after BI, or HAECs (1.5×10^5 cells/100-mm dish) were seeded in the complete medium supplemented

with 10% FBS. After 24 h, medium was replaced with fresh complete medium supplemented with 10% FBS and various concentrations of ALA (0, 0.5, 1, 2 and 4 mmol/L) and cells were incubated for 72 h. To inhibit activity of p38 MAPK or ERK1,2, VSMCs were pretreated with SB203580 (10 μmol/L) or PD98059 (30 μmol/L) for 1 h before ALA treatment (2 mmol/L, unless otherwise stated), respectively. For siRNA transfection, a reverse transfection procedure was employed. Briefly, after trypsinization, VSMCs were transfected with 100 nmol/L of Nur77-siRNA (sense:5'-GUGUUGAUGUUCCUGCCUUdTdT-3') or control siRNA (Con-siRNA) duplexes (sense:5'-CCUACGCCACCAAUUUCGUdTdT-3') using Lipofectamine RNAiMAX (Invitrogen, Carlsbad, CA) according to the manufacturer's instruction. Twenty four hours after transfection, cells were incubated in fresh complete medium with or without ALA (2 mmol/L, unless otherwise stated) for 72 h. Floating cells and adherent cells detached by trypsinization were collected and washed with ice-cold PBS. Cells were fixed with 70% ethanol at -20°C for overnight, then incubated with propidium iodide (40 mg/ml), RNaseA (10 μg/ml) and 0.1% NP-40 for 30 min at 37°C and analyzed with a FACSCallbur (BD Biosciences, San Jose, CA). DNA histogram analysis was performed using the CellQuest software (BD Biosciences).

Plasmids

Nur77 expression vector (pECE-Nur77) and the reporter plasmids, NurRE-Luc which contains 3 copies of Nur77 binding sites from POMC gene promoter (3), Nur77 promoter luciferase (Nur77 pro-Luc) (4) and pNF-κB-Luc (5) were described previously.

Transient transfection assay and siRNA transfection.

HepG2 cells and VSMCs were cultured in MEM and DMEM supplemented with 10% FBS, respectively. For luciferase assay, HepG2 (8×10^4) were seeded in 24-well plates and

incubated in complete medium for 24 h. HepG2 were transfected with 200 of NurRE-Luc, and 100 of pECE-Nur77 using TransIT-LT1 transfection reagent (Mirus Bio Incorporation, Madison, WI) according to the manufacturers' instructions. VSMCs cells (3×10^5) were transfected with 800 ng of NurRE-Luc with or without 600 ng of pECE-Nur77 or 1 μg of Nur77 pro-Luc or NF-κB-Luc with or without Nur77-siRNA (100 nmol/L) in 12-well plates using Amaxa Nucleofector kit (Amaxa Biosystem, Cologne, Germany) according to the manufacturers' instructions. Cytomegalovirus (CMV)-β-galactosidase plasmids were cotransfected as an internal control. Twenty four (HepG2) or six (VSMCs) hours after transfection, cells were treated with ALA for 24 h (HepG2) or ALA (2 mmol/L) and TNF-α (10 ng/mL) for 18 h and harvested for luciferase and β-gal assays. Luciferase activity was normalized to the β-galactosidase activity. For siRNA transfection, a reverse transfection procedure was employed. Briefly, after trypsinization, VSMCs (2×10^4 cells/cm^2) were seeded in 100-mm dishes and transfected with Nur77-siRNA (100 nmol/L) or control scramble siRNA (Con-siRNA) duplexes using Lipofectamine RNAiMAX (Invitrogen) according to the manufacturer's instruction. Twenty four hours after transfection, cells were serum starved for 24 h, then incubated in fresh complete medium containing ALA for 2 h and harvested for Western Blotting.

TUNEL assay

VSMCs (1.4×10^4 cells/cm^2) were plated into 8-well culture slide and incubated in complete medium supplemented with 10% FBS. After 24 h, cells were treated with fresh complete medium containing ALA for 24 h and fixed with 2% paraformaldehyde in PBS for 1 h. Using In situ Cell Death Detection Kit (Roche, Basel, Switzerland), fragmented DNA in the apoptotic cells were labeled according to the manufacturer's instruction. Labeled cells were visualized directly by fluorescence microscopy.

Casepase-3-like (DEVDase) activity assay

VSMCs (1.4×10^4 cells/cm^2) were incubated in complete medium for 24 h. Cells were then treated with fresh complete medium containing ALA for indicated times and enzymatic activities of DEVDase (Casepase-3 activity) were determined by incubating 60 μg of cell lysates in 100 μl reaction buffer (1% NP-40, 20 mmol/L Tris–HCl, pH 7.5, 137 mmol/L NaCl, and 10% glycerol) containing 5 μmol/L of chromogen substrate [Asp-Glu-Val-Asp-p-nitroanilide (DEVD-pNA)] (Sigma) at 37°C for 2 h. The release of chromophore p-nitroanilide (pNA) was monitored spectrophotometrically (405 nm).

Semi-quantitative RT-PCR analyses

VSMCs (7.5×10^5 cells) were plated in 100-mm culture dishes in complete medium. After 24 h, cells were incubated in fresh complete medium with or without ALA for indicated times. To investigate the effect of inhibitors of various signal transduction pathways on ALA-induced Nur77 expression, VSMCs were pretreated with indicated concentrations of various inhibitors for 1 h prior to ALA treatment for 20 h and harvested for total RNA isolation using TRIzol reagent (Invitrogen, Carlsbad, CA). For semi-quantitative RT-PCR, 2 μg of total RNA was used to synthesize the first strand cDNA using the First Strand cDNA synthesis kit (Fermentas, EU). The first strand cDNAs were amplified by PCR according to the following PCR parameters: 94°C for 30 s, 59°C for 30 s, and 72°C for 30 s, 25 cycles. Primers used in the PCR were as follows: Nur77 forward, 5'-GCTCATCTTCTG CTCAGGCCT-3' and reverse, 5'-CAGACGTGACAGGCAGCTGGC-3'; and β-actin forward, 5'-GGCATCGTCACCAACTGGGAC-3' and reverse, 5'-CGATTTCCCGCTCGG CCGTGG-3'.

Western blot and co-immunoprecipitation analyses

VSMCs (7.5×10^5 cells) were plated into 100-mm culture dishes and incubated in complete medium. After 24 h, cells were treated with fresh complete medium containing ALA (2 mmol/L) for indicated times. Whole cell lysates were prepared using a lysis buffer (20 mmol/L Tris-HCl, pH 7.4, 10 mmol/L Na_4P_2OH, 100 mmol/L NaF, 2 mmol/L Na_3VO_4, 5 mmol/l EDTA, pH 8.0, 0.1 mmol/L PMSF, 1% NP-40) containing proteinase and phosphatase inhibitors. To detect cytosolic release of cytochrome c, cytosolic extracts free of mitochondria were prepared by lysing cells for 2 min using a lysis buffer (250 mmol/L sucrose, 1 mmol/L EDTA, 20 mmol/L Tris-HCl, pH 7.2, 1 mmol/L dithiothreitol, 10 mmol/L KCl, 1.5 mmol/L $MgCl_2$, 5 μg/ml pepstatin A, 10 μg/ml leupeptin, 2 μg/ml aprotinin). Lysates were centrifuged at 12,000 *g* at 4°C for 10 min to obtain the supernatant (cytosolic extracts) and the pellet (mitochondria). Whole cell lysates or cytosolic extracts were resolved by SDS-PAGE and transferred to Immobilon-P-membrane (Millipore, Billerica, MA). After blocking, the membrane was incubated with various primary antibodies, including mouse monoclonal anti-β-actin (A5441) antibody (Sigma), mouse monoclonal anti-Bax (B-9) and anti-Bcl-2 (C-2) antibodies (Santa Cruz Biotechnology, Santa Cruz, CA), mouse monoclonal anti-Nur77, anti-cytochrome c antibodies (BD Biosciences), rabbit polyclonal anti-p38 MAPK, anti-phospho p38 MAPK, anti-ERK 1,2 (p44/42), anti-phospho ERK (Thr201/ Tyr204), anti-JNK and anti-phospho JNK (Thr183/Tyr185) antibodies (Cell Signaling Technology, Beverly, MA). After washing with TBST three times, the membranes were incubated with horseradish peroxidase (HRP)-conjugated secondary antibodies and signals were detected using the ECL Western blotting detection system (Amersham, Buckinghamshire, UK). For co-immunoprecipitation assay, whole cell lysates treated with ALA were immunoprecipitated using anti-Nur77 antibody (Santa Cruz Biotechnology, M-210) and the immune complex was subjected to Western blotting with anti-Bcl-2 antibody.

Immunocytochemistry and Immunofluorescence analyses *in vitro*

Cells were seeded on cover slip glasses at a density of 1.4×10^4 cells/cm^2 in complete medium and allowed to attach for 24 h. Cells were incubated in fresh complete medium with or without ALA (2 mmol/L) for indicated times and fixed with 4% paraformaldehyde for 15 min at room temperature. Fixed cells were permeablized with 0.2% Triton X-100 in PBS for 15 min on ice and incubated with anti-Nur77 (C-19) antibody (Santa Cruz Biotechnology) for overnight at 4°C followed by Polink-2 Plus HRP Anti-Goat DAB Detection kit (Golden Bridge International, Inc., Mukilteo, WA).

For immunofluorescence, fixed cells were incubated with anti-Nur77 (C-19) antibody (Santa Cruz Biotechnology) and anti-Hsp60 antibody (BD Biosciences), followed by further incubation with Alexa Fluor-488-labeled anti-goat secondary antibody (Invitrogen) and Alexa Fluor-568-labeled anti-mouse secondary antibody (Invitrogen), respectively for 3 h at room temperature. Cell nuclei were stained with DAPI (5 μg/mL) and mounted. Samples were analyzed using an inverted MRc5 Carl Zeiss fluorescence microscopy (Thornwood, NY).

Preparation of adenoviruses

To downregulate Nur77 expression, adenovirus encoding short hairpin RNA (shRNA) against rat Nur77 (Ad-shRNA) was generated. Briefly, annealed oligonucleotides targeting Nur77 were cloned into pRNATH1.1/Adeno shuttle vector (GenScript Co., Piscataway, NJ), which contains a GFP marker under the control of CMV promoter. The pRNAT-H1.1/Adeno-shNur77 or pRNATH1.1/Adeno vector alone (control adenovirus; Ad-shRNA) was electroporatically transformed into BJ5138 cells containing pAdeasy-1 adenoviral vector and recombinant adenoviral plasmids were generated by homologous

recombination using AdEasy Adenoviral Vector system (Stratagene, La Jolla, CA), according to the manufacturer's instructions. The recombinant adenoviral plasmids were transfected into low-passage HEK-293 cells after *Pac*I digestion and virus generation was confirmed by the appearance of a cytopathic effect and by GFP expression. Adenoviruses were amplified in HEK-293 cells and purified by CsCl gradient centrifugation. The viruses were collected and desalted, and the titers were determined using Adeno-X Rapid titer (BD Biosciences).

Balloon-injury (BI) of the rat carotid artery model and delivery of adenoviruses into injured arteries

Balloon injury (BI) of the rat carotid artery was performed as described previously (6, 7). Briefly, 8-week-old male SD rats were anesthetized with 50 mg/kg of sodium pentobarbital (Entobar; Hanlim Pharmaceutical, Yong-In, Korea) and a balloon catheter was introduced through the right external carotid artery into the aortic arch. The carotid artery was damaged by passing the inflated balloon catheter back and forth through the lumen. To deliver adenovirus expressing shRNA against Nur77 (Ad-shNur77) or control adenovirus (Ad-shRNA), 10 μl (10^{11} pfu/ml) of Ad-shRNA or Ad-shNur77 in PBS were infused into injured artery for 15 min immediately after BI. ALA (50 or 100 mg/kg/day) or saline (vehicle) was administered by intraperitoneal injection once a day, starting from 3 days before to 14 days after injury, and animals were sacrificed at 14 days after injury.

Histological and morphometric analyses

Histological and morphometric analyses were performed as described previously (6, 7). At the end of each experiment, rats were euthanized by intravenous pentobarbital overdose. Right and uninjured left common carotid arteries were removed, fixed overnight in

4% formaldehyde in PBS and paraffin-embedded. Serial cross sections (4 μm thick) of carotid arteries were stained with hematoxylin and eosin (H&E) and analyzed using iSolution DT Ver 7.7 imaging software (IMT i-Solution Inc., Coquitlam, Canada), to determine the intimal area (IA) and medial area (MA) and to calculate the intima to media ratio.

Immunohistochemistry and TUNEL analysis

Immunohistochemical staining was performed as described previously (5). Briefly, cross sections (4 μm thick) of uninjured (control) or balloon-injured rat carotid arteries were deparaffinized, rehydrated and antigen retrieval was carried out by microwave oven heating in 0.01 M sodium citrate buffer (pH 6.0). Sections were then incubated with goat polyclonal anti-Nur77 (C-19) antibody (Santa Cruz Biotechnology) or mouse monoclonal anti-CD31/PECAM-1 antibody (Millipore, MAB1393, 1:50 dilution) followed by Polink-2 Plus HRP Anti-Goat DAB Detection kit (Golden Bridge International, Inc., Mukilteo, WA) or UltraVision LP Detection System HRP Polymer & DAB Plus Chromogen (Thermo Fisher Scientific Inc., Fremont, CA), respectively, according to the manufacturers' instructions.

TUNEL assays were performed using ApopTag Peroxidase *In Situ* Apoptosis Detection kit (Millipore) according to manufacturer's instructions. In brief, control and injured carotid artery sections were deparaffinized, rehydrated and digested by proteinase K method. Sections were then incubated with fresh 3% hydrogen peroxide for 10 min, washed with PBS-Tween 20, incubated with TUNEL reaction mixture containing terminal deoxynucleotidyl transferase (TdT) and digoxigenin-conjugated dUTP for 1 h at 37°C followed by incubation of anti-digoxigenin conjugate (peroxidase) and DAB kit solution.

Transmission electron microscopy (TEM)

To detect apoptosis in VSMCs, transmission electron microscopy was performed as previously described (8). Briefly, right and uninjured left common carotid arteries were removed from rats given ALA (100 mg/kg/day) from 3 days before injury to 10 days after balloon injury. Arteries were fixed overnight in a phosphate buffer containing 4% paraformaldehyde and 1% glutaraldehyde. The specimen were postfixed in 1% osmium tetroxide, dehydrated, and embedded in epoxy resin. Ultrathin sections were stained with 1% uranyl acetate and analyzed with a Philips CM200 transmission electron microscope.

BrdU incorporation assay

To determine the effect of ALA on HAEC proliferation, BrdU incorporation was performed as previously described (9). HAECs (5×10^3) were seeded in 96-well plates and incubated with culture medium containing 0.5% FBS for 24 h. Cells were stimulated with 10% FBS for 16 h and incubated with BrdU labeling solution for an additional 2 h. The BrdU incorporation was analyzed using 5'-Bromo-2'-deoxy-uridine Labeling and Detection Kit III (Roche, Indianapolis, IN) according to manufacturer's instructions.

Platelet aggregation assay

To prepare the platelet-rich plasma (PRP), whole blood collected from human volunteers who had provided informed consent was anticoagulated with sodium citrate (3.8% final concentration) and centrifuged at 1,000 rpm for 10 minutes at room temperature. Platelet-poor plasma (PPP) was obtained by centrifuging the remaining blood fraction for 10 minutes at 3,000 rpm. PRP (250 μL) was incubated in glass cuvettes for at least 5 minutes. The baseline was set to the light transmission of nonstirred PRP against PPP. PRP was incubated with ALA (0, 100, 200, 300 μmol/L, final concentration) for 2 min and then activated with arachidonic acid (1 mmol/L, final concentration). Platelet aggregation was

assessed by measuring changes in light transmission during constant stirring of the samples (1,000 rpm) using a chrono-Log lumi-aggregometer (model 490-4D, Chrono-Log, Havertown, Pennsylvania).

Statistical analysis

Results are expressed as means ± SE (n=3-5). Data were analyzed with one-way analysis variance of ANOVA followed by a post hoc least significant difference test. A value of $P < 0.05$ was considered statistically significant. All experiments were performed at least three times.

References

1. Ahn JD, Morishita R, Kaneda Y, Lee SJ, Kwon KY, Choi SY, Lee KU, Park JY, Moon IJ, Park JG, Yoshizumi M, Ouchi Y, Lee IK. Inhibitory effects of novel AP-1 decoy oligodeoxynucleotides on vascular smooth muscle cell proliferation in vitro and neointimal formation in vivo. *Circ Res.* 2002;90:1325-1332.
2. Walker LN, Bowen-Pope DF, Ross R, Reidy MA. Production of platelet-derived growth factor-like molecules by cultured arterial smooth muscle cells accompanies proliferation after arterial injury. *Proc Natl Acad Sci U S A.* 1986;83:7311-7315.
3. Yeo MG, Yoo YG, Choi HS, Pak YK, Lee MO. Negative cross-talk between Nur77 and small heterodimer partner and its role in apoptotic cell death of hepatoma cells. Mol Endocrinol. 2005;19:950-963.
4. Song KH, Park JI, Lee MO, Soh J, Lee K, Choi HS.LH induces orphan nuclear receptor Nur77 gene expression in testicular Leydig cells. Endocrinology. 2001 Dec;142(12):5116-23.
5. Kim HJ, Yoo EK, Kim JY, Choi YK, Lee HJ, Kim JK, Jeoung NH, Lee KU, Park IS, Min BH, Park KG, Lee CH, Aronow BJ, Sata M, Lee IK. Protective role of clusterin/apolipoprotein J against neointimal hyperplasia via antiproliferative effect on vascular smooth muscle cells and cytoprotective effect on endothelial cells. Arterioscler Thromb Vasc Biol. 2009 ;29:1558-1564.
6. Lee KM, Park KG, Kim YD, Lee HJ, Kim HT Kim, Cho WH, Kim HS, Han SW, Koh GY, Park JY, Lee KU, Kim JG, Lee IK. Alpha-lipoic acid inhibits fractalkine expression and prevents neointimal hyperplasia after balloon injury in rat carotid artery. *Atheroscelrosis.* 2006;189:106-114.
7. Ahn JD, Morishita R, Kaneda Y, Lee SJ, Kwon KY, Choi SY, Lee KU, Park JY, Moon IJ, Park JG, Yoshizumi M, Ouchi Y, Lee IK. Inhibitory effects of novel AP-1

decoy oligodeoxynucleotides on vascular smooth muscle cell proliferation in vitro and neointimal formation in vivo. *Circ Res.* 2002;90:1325-1332.

8. Lee WJ, Lee IK, Kim HS, Kim YM, Koh EH, Won JC, Han SM, Kim MS, Jo IH, Oh GT, Par IS, Youn JH, Park SW, Lee KU, Park JY. Alpha-lipoic acid prevents endothelial dysfunction in obese rats via activation of AMP-activated protein kinase. *Arterioscler Thromb Vasc Biol*. 2005;25:2488-2494.
9. Kim SY, Jeoung NH, Oh CJ, Choi YK, Lee HJ, Kim HJ, Kim JY, Hwang JH, Tadi S, Yim YH, Lee KU, Park KG, Huh S, Min KN, Jeong KH, Park MG, Kwak TH, Kweon GR, Inukai K, Shong M, Lee IK. Activation of NAD(P)H:quinone oxidoreductase 1 prevents arterial restenosis by suppressing vascular smooth muscle cell proliferation. *Circ Res*. 2009;104:842-850.

Supplemental Figure Legends

Supplemental Fig. I. ALA induces G0/G1 phase cell cycle arrest in VSMCs. FACS analysis. VSMCs (7.5×10^5 cells/100-mm culture plates) were serum starved for 48 h and incubated with fresh medium containing 10% FBS and ALA (0, 0.5, 1, 2 and 4 mmol/L) for 22 h. Floating cells and adherent cells were collected and stained with propidium iodide (PI). Cell cycle distribution was analyzed by flow cytometry.

Supplemental Fig. II. ALA induces apoptosis more potently in proliferating than quiescent VSMCs. FACS analysis. VSMCs were seeded in complete medium and incubated for 24 h. The medium was replaced with fresh medium containing 10% or 0.5% FBS in the presence or absence of ALA (1 mmol/L) and cells were incubated for 72 h. Floating cells and adherent cells were collected, stained with propidium iodide (PI) and analyzed by flow cytometry. The M1 (sub G1) cell population represents apoptotic cells.

Supplemental Fig. III. ALA represses transcriptional activity of Nur77. HepG2 cells (A) and VSMCs (B) were transiently transfected with NurRE-Luc together with or without pECE-Nur77 expression plasmid. Twenty four (HepG2) or six (VSMCs) hours after transfection, cells were incubated in fresh complete medium with various concentrations of ALA as indicated for 24 h (HepG2) or 18 (VSMCs) h, and harvested for luciferase and β-galactosidase assays. Luciferase activity was normalized against β-galactosidase activity and plotted as fold change relative to basal luciferase activity of NurRE-Luc reporter alone. (A) $*P < 0.001$ versus reporter alone, $**P < 0.01$, $^{\#}P < 0.005$ versus Nur77-stimulated activity without ALA treatment. (B) $*P < 0.005$ versus reporter alone, $**P < 0.05$ versus Nur77-stimulated activity without ALA treatment.

Supplemental Fig. IV. ALA significantly diminished intimal area and intima to media ratio in carotid arteries at 14 days after balloon injury (BI). The morphometric analyses of cross-sections of carotid arteries isolated from rats that were given intraperitoneally either saline (vehicle) or ALA (50 or 100 mg/kg/day) daily from 3 days before to 14 days after BI. (A) Medial area was calculated by subtracting the area defined by the internal elastic lamina from the area defined by the external elastic lamina, and intimal area was determined as the area defined by the luminal surface and the internal elastic lamina. (B) The ratio of intima to media was calculated (n = 6 per group, $^{*}P < 0.001$ versus uninjured control group, $^{**}P < 0.01$, $^{\#}P < 0.005$ versus balloon-injured group treated with saline.

Supplemental Fig. V. Transmission electron microscopy of carotid arteries 10 days after balloon injury (BI). Transmission electron microscopic examination was performed on the sections of control uninjured (a, c) and balloon-injured (b, d) carotid arteries of rats given saline (a, b) or ALA (c, d, 100 mg/kg/day) daily from 3 days before injury to 10 days after BI. Representative photographs showing VSMCs present in the medial (a, c) and neointimal (b, d) areas in uninjured (a, c) and balloon-injured (b, d) carotid arteries. A typical nuclear fragmentation is indicated by arrowheads (d). Scale bar indicates 1 μm (magnification × 5,000).

Supplemental Fig. VI. Adenovirus-mediated downregulation of Nur77 significantly reduced inhibitory effect of ALA on intimal thickening. Morphometric analysis of the sections of carotid arteries from rats that were infused with Ad-shNur77 or Ad-shRNA (control) immediately after BI and intraperitoneally injected with either saline or ALA (100 mg/kg/day) daily from 3 days before to 14 days after BI. (A) Intimal and medial areas.

Medial area was calculated by subtracting the area defined by the internal elastic lamina from the area defined by the external elastic lamina, and intimal area was determined as the area defined by the luminal surface and the internal elastic lamina. (B) The ratio of intima to media. *$P < 0.001$ versus uninjured group, **$P < 0.005$ versus balloon-injured group treated with saline, $^{\#}P < 0.01$ versus Ad-shRNA-infused group treated with ALA ($n = 6$ per group).

Supplemental Fig. VII. Nur77 siRNA reversed inhibitory effect of ALA on TNF-α-stimulated NF-κB activity. VSMCs were transiently transfected with pNF-κB-Luc reporter plasmid with 100 nmol/L of Nur77-siRNA (siNur77). Six hours after transfection, cells were incubated in fresh complete medium with ALA 1 h prior to TNF-α (10 ng/mL) treatment for 18 h, and harvested for luciferase and β-galactosidase assays. Luciferase activity was normalized against β-galactosidase activity and plotted as fold change relative to basal luciferase activity of NF-κB-Luc reporter alone. *$P < 0.001$ versus reporter alone, **$P < 0.01$ versus TNF-α-stimulated activity without ALA, $^{\#}P < 0.05$ versus TNF-α and ALA treatment.

Supplement Material

Supplemental Fig. I

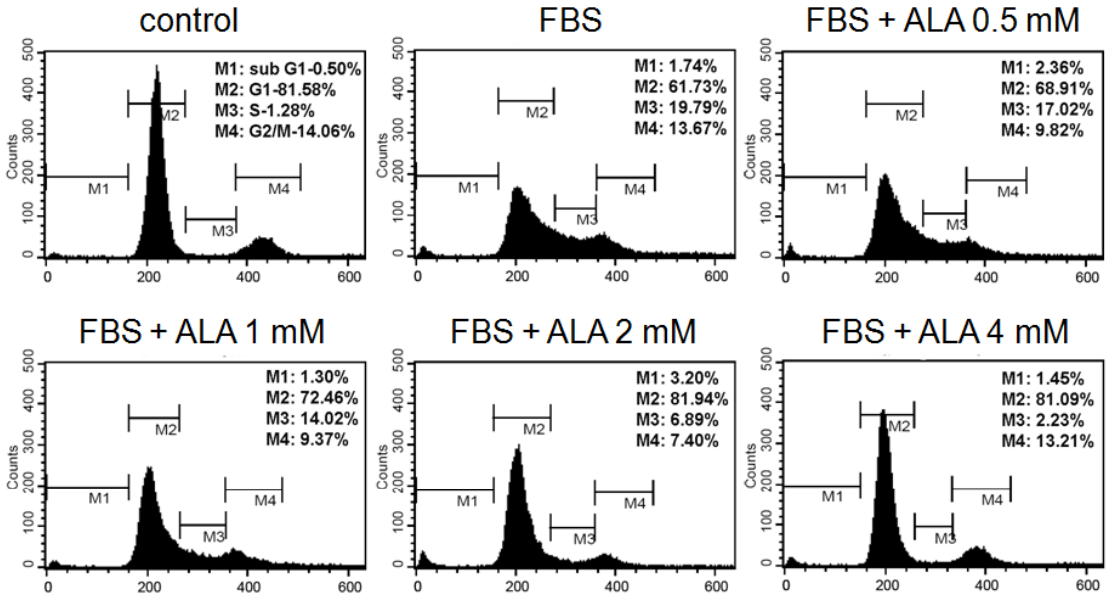

Supplemental Fig. II

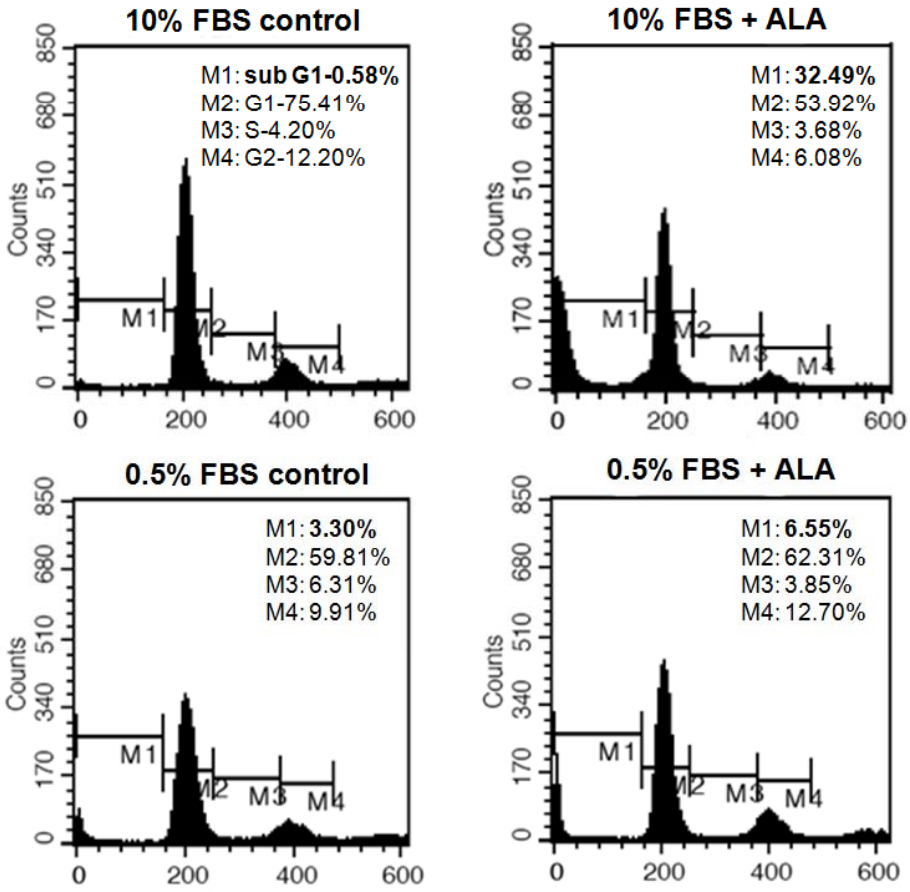

Supplemental Fig. III

A

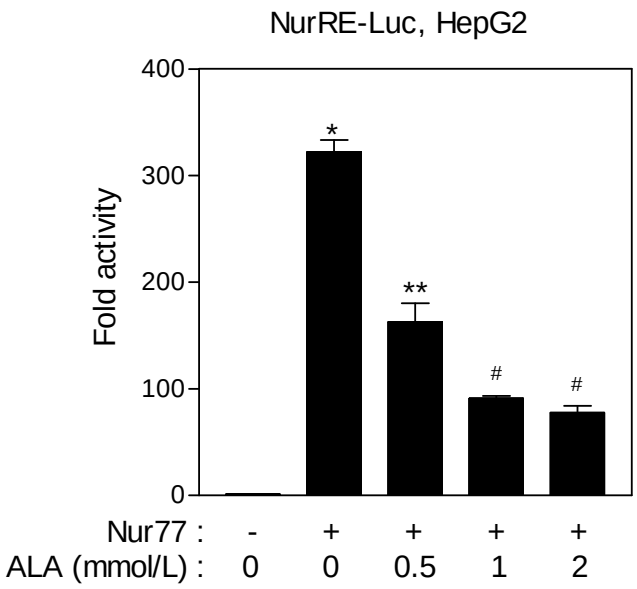

B

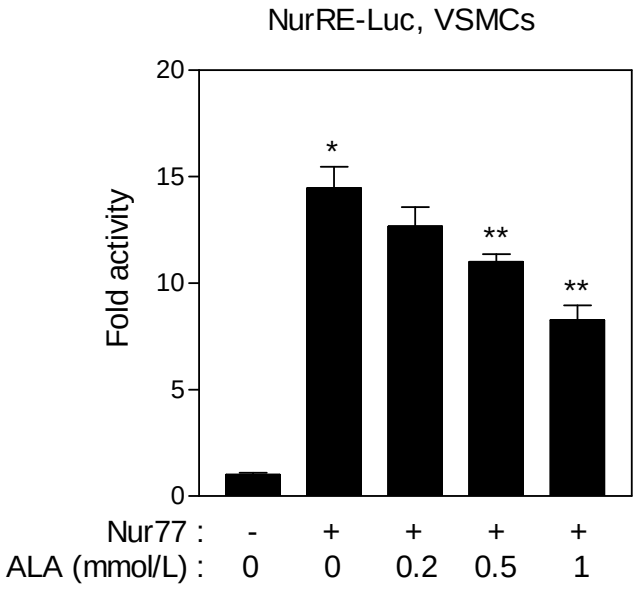

Supplemental Fig. IV

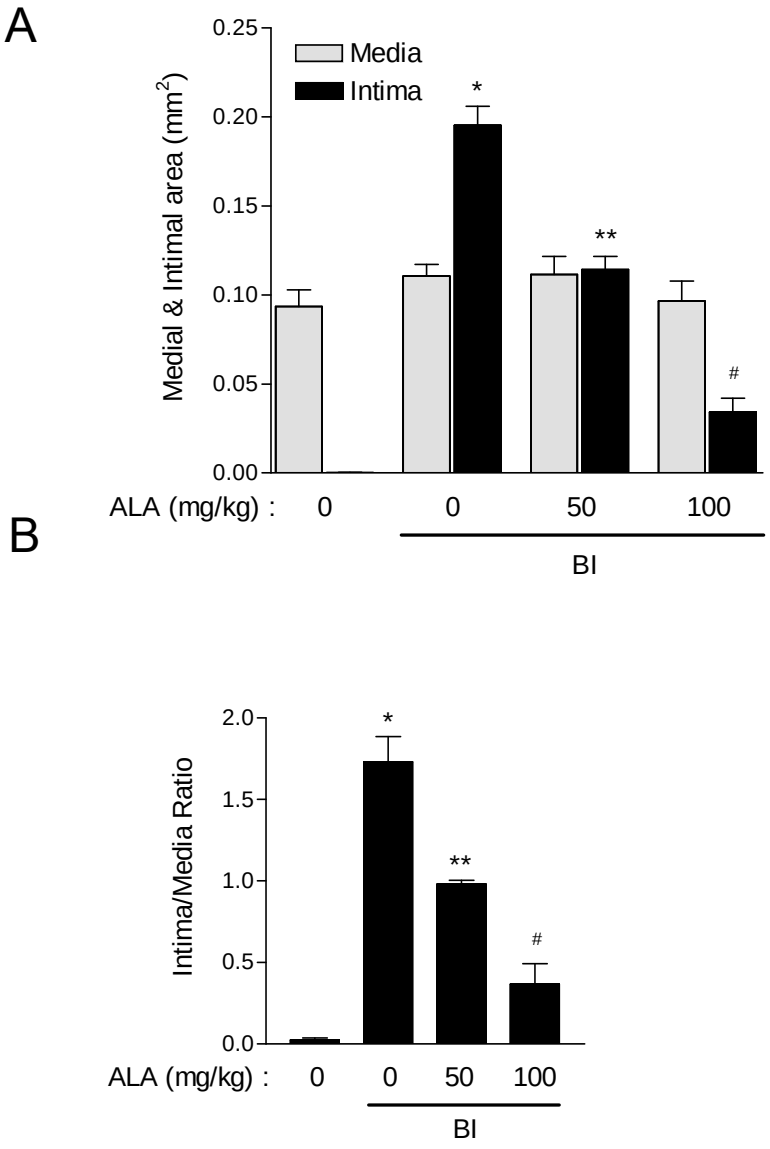

Supplemental Fig. V

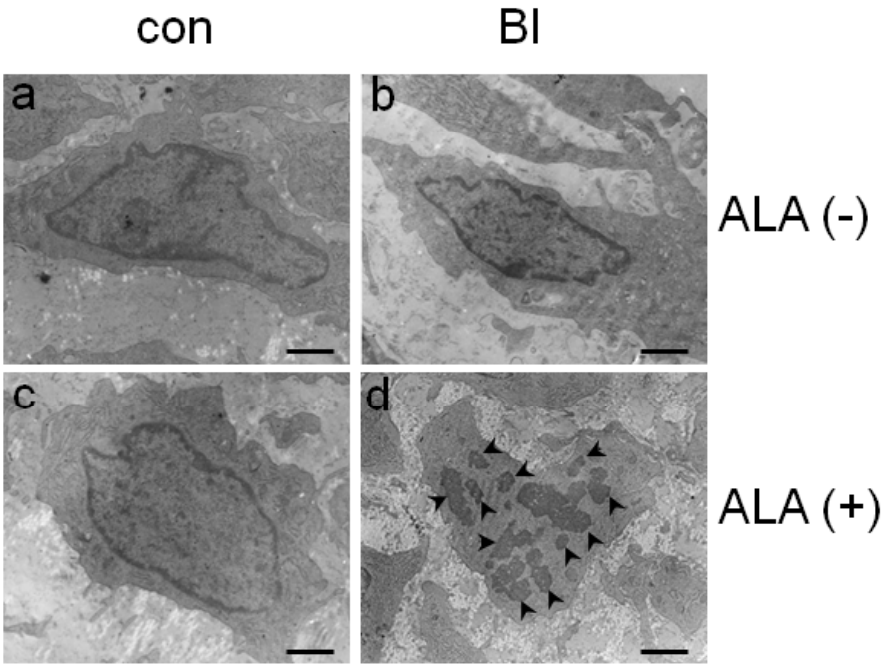

Supplemental Fig. VI

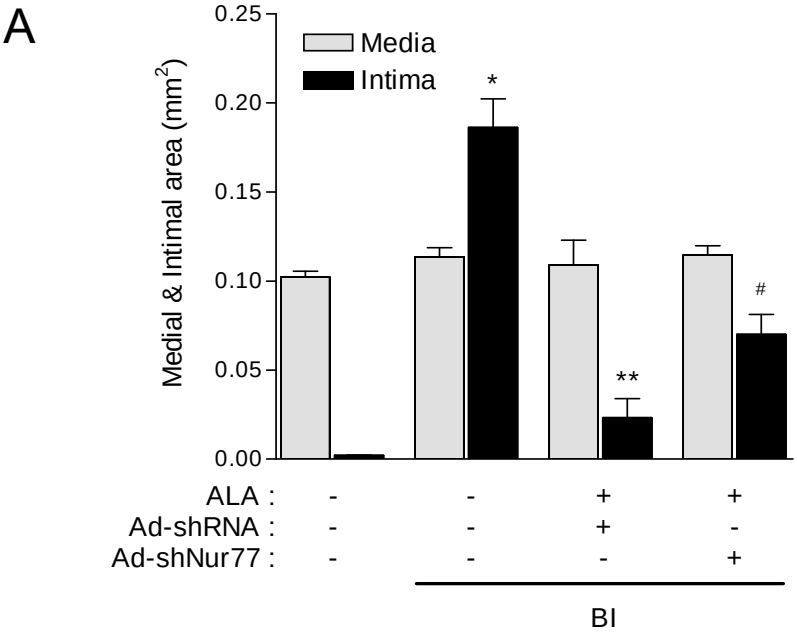

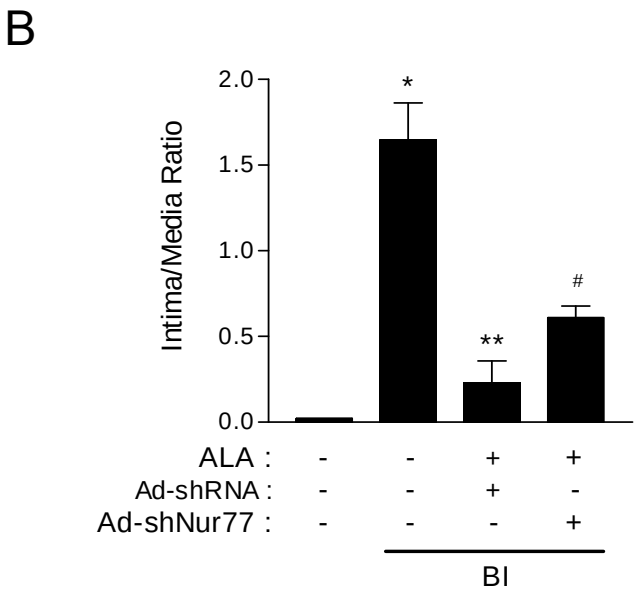

Supplemental Fig. VII